

Focused ion beam sample preparation for atom probe tomography

Author:

McKenzie, Warren Richard; Emmanuelle, Marquis; Paul, Munroe

Publication details:

Microscopy: Science, Technology, Applications and Education

Publication Date:

2010

License:

<https://creativecommons.org/licenses/by-nc-nd/3.0/au/>

Link to license to see what you are allowed to do with this resource.

Downloaded from <http://hdl.handle.net/1959.4/45631> in <https://unsworks.unsw.edu.au> on 2024-03-28

Focused ion beam sample preparation for atom probe tomography

W.R. McKenzie¹, E.A. Marquis², and P.R. Munroe¹

¹Electron Microscope Unit, University of New South Wales, NSW 2052, Australia

²Department of Materials, Oxford University, Parks Road, Oxford OX1 3PH, UK

Atom Probe (AP) tomography is maturing into a routine method for the atomic resolution compositional analysis of metals, semiconductors and some polymers. This is often combined with a Transmission Electron Microscope (TEM) analysis of the same region of interest. The Focused Ion Beam (FIB) microscope has evolved as an essential tool for site and orientation specific sample preparation for such analysis. We review existing FIB-based AP/TEM sample preparation techniques and present a number of innovative approaches to specimen preparation illustrated with examples including a silicon-on-insulator semiconductor device, a twin boundary in a Cu-Bi alloy and a crystalline precipitate phase in a bulk metallic glass.

Keywords Atom probe tomography; APT; focused ion beam; FIB; Transmission Electron Microscope; TEM.

1. Atom probe tomography

Atom probe tomography (APT) is a microstructural characterisation technique that uses the principle of field ion evaporation to remove individual atoms from a sample by applying a high electric field to the region of interest, which is in the shape of a sharpened tip. As described in the schematic Fig. 1(a), atoms are removed from the specimen with the aid of a field spike created by a voltage pulse from the local electrode, and (or) a laser pulse focussed on the specimen tip. The species of each individual atom is identified with the aid of a “delay line detector”, a time-of-flight mass-spectrometer. The position of the atom, in the plane perpendicular to the axis of the specimen, is derived from the location of the atom when it impacts the detector which is position sensitive comprising of an array of “micro-channels” over its area. The z-coordinate (parallel to the axis of the specimen) is determined by the atoms order in the evaporation sequence.

The atom’s identity and co-ordinates are then recorded to produce a data set which can be reconstructed into 3-dimensional volumes [1], such as that shown in Fig. 1(b). As the results are based on electronic data, the data set can also be studied using statistical analysis. As a microstructural characterization technique, it has the highest spatial resolution of any method known, and has a compositional sensitivity in the order of parts per million. The atom-probe tomography technique has been reviewed in several books [2-3] and review articles [1, 4].

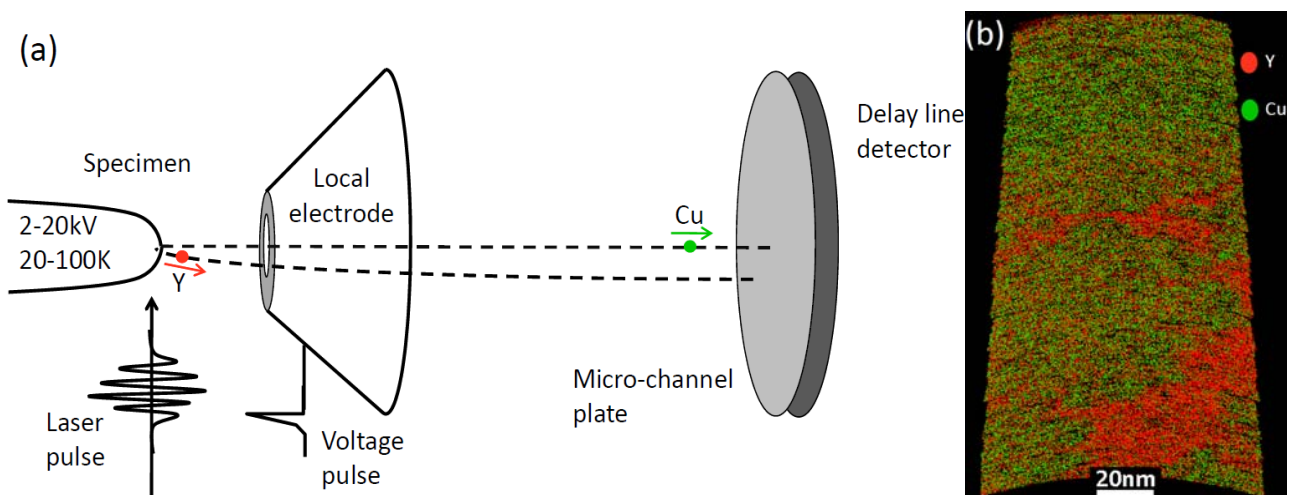


Fig. 1: (a) Schematic of the geometry of the Local Electrode Atom Probe (LEAP). (b) 3D reconstruction from a Mg-Y-Cu bulk metallic glass [5]. Y atoms are shown in red, Cu in green (Mg has been omitted for clarity) which show a clear segregation of the species into two metastable metallic glass phases. Preparation of this specific sample is described in section 4.4.1.

For many atom probe-based problems, transmission electron microscope (TEM) analysis complements these studies by providing scaled projection images of the samples, which are more intuitive to interpret, and contain crystallographic information that cannot be easily or accurately obtained with APT. In addition, a preliminary TEM analysis of an APT sample is often required to determine if a feature of interest is located in the corresponding small volume of an atom probe post.

To induce field ion evaporation and collect atom probe data, a voltage gradient at the tip in the order of 20-40 V/nm is required. This is achieved by applying a voltage between the local electrode and sample up to about 10 to 20 kV. Under these conditions, electric fields can only be obtained if the sample is formed into the shape of needle with a very sharp tip. The required geometries for such samples to achieve field ion evaporation are as follows [6]:

- Needle-shaped,
- Uniform circular cross-section – to produce a radially symmetric electric field around the tip
- Small taper angle $< 5^\circ$
- Tip radius typically < 50 nm – to produce a sufficiently high electric field at the tip to allow field ion evaporation
- Conductive path to the tip
- Minimal damage introduced to the tip during specimen preparation – the apex region of the needle has to be representative of the original sample.

The dimensions of analysed volumes are of the order of 50 nm x 50 nm x 20-500 nm; the depth depending on the quality of the specimen and position of features of interest. Fig. 2 taken from the literature [7] illustrates the actual size of the specimen as imaged by TEM (a) compared to the reduced volume analysed by atom-probe tomography (b).

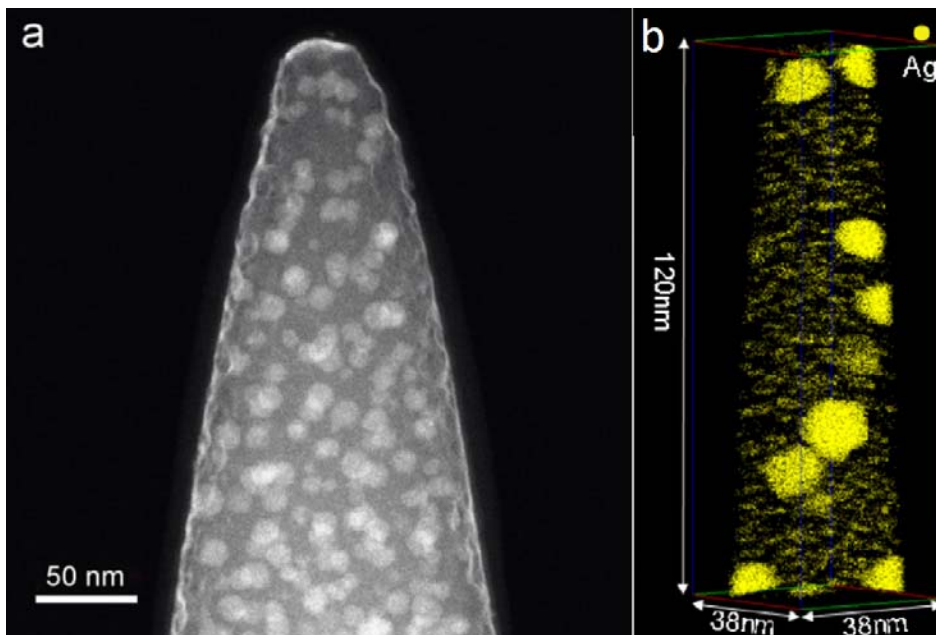


Fig. 2 [7]: (a) TEM image of an Ag-Al alloy specimen (b) analysed atom probe dataset of the same specimen. Note that the edges of the specimen fall outside the detector and therefore are not analysed.

Until the development of fast low energy laser pulsers, analyses via atom probe tomography (or the similar technique of field ion microscopy) were restricted to conducting materials that could be made in the shape of sharp needles by electropolishing [8]. Laser pulsing has revolutionized the field of applications of APT by enabling the analysis of semiconductors [4] and insulator materials. These materials, however, cannot be easily shaped into sharp needles. Isolated attempts have been made on non-metallic materials including GaAs [9], GaIn [10], SiC [11], or Si prepared in the form of electropolished needles [12] or as grown whiskers [13]. The disadvantage of electropolishing is the high difficulty in selecting specific features within a microstructure. Back polishing methods have been developed to prepare specimens with selected features within 50nm from the apex [14]. Combining electron microscopy observation of specimens using appropriate holders [15] and short pulse polishing, grain boundaries or particles can be positioned within the field of view of an atom-probe tomography analysis [16]. Other attempts at producing sharp needles have used broad ion beam etching, such as that demonstrated by Walls et al. [17] and Larson et al. [18]. These procedures can, however, be tedious and are generally not applicable to complex multiphase structures.

The development of the Focused Ion Beam system has provided an alternative and very versatile means of creating atom probe samples and has broadened the application base of atom probe tomography significantly allowing the analyses of non-conductive materials and site specific regions. Most atom probe laboratories are now equipped with a FIB system as a routine sample preparation tool.

2. Focused Ion Beam Microscope

The Focused Ion Beam instrument, generally, operates in a similar way to a scanning electron microscope, with the major difference being that ions, usually Ga^+ , are used to interact with the surface, rather than electrons, to produce a secondary electron signal for imaging. As the ions have a much larger mass than the electrons, the ion beam has the capability of sputtering away atoms interacting with the beam allowing the FIB to be used as a milling tool if high ion currents are selected.

One other fundamental capability of the FIB is the ability to utilize gas chemistries to induce ion beam-assisted chemical vapour deposition. Depositions of tungsten, platinum and amorphous carbon are the common materials deposited as a protective layer for the sample surface when milling near sensitive areas, and where ion beam overspray may otherwise affect the sample.

The dual beam FIB contains an electron column, as well as the ion column, which images at an angle (typically 52°) to the ion beam. This allows the user to image the sample in-situ while it is being milled. Site specific sample preparation techniques, some of which will be described, rely on the ability to image while milling.

As with any electron or ion microscope, dual beam FIB's can also be interfaced with other components. In the context of FIB preparation of samples for APT an *in-situ* micromanipulator is one of the most important, as it is capable of transferring a small segment of a sample from its bulk to a mount on an atom probe post.

A number of FIB-based preparation techniques have been developed to create atom-probe posts for specific scenarios. The most common types are reviewed or presented in this paper: specifically, the Moat, Liftout, Micropost release, and Encapsulation techniques. All of these methods involve the fabrication of a post, and are all finished with a procedure known as annular milling to sharpen the tip to the appropriate radii.

3. Annular Milling

Annular milling is a procedure where a pre-prepared post is milled directly from above (anti-parallel to the axis of the post) to sharpen the tip containing the region of interest (ROI) and has been described elsewhere by many authors [19-22]. The pattern used is radial in shape with an outer diameter slightly larger than that of the needle (or post) and an inner diameter (inside which no material is removed) larger than the inner radius required for the tip.

The pattern may be generated by FIB software rastering the ion probe in the shape of an annulus. The use of an annulus with a graded intensity profile has also been investigated to optimize the shape of the microposts shank [23]. Patterning using this regime is achieved with bitmap image files which can be used to control the patterning in some FIB user interface programs.

Annular milling is performed using a number of steps with progressively lower ion currents, and inner radii, until the required dimensions are reached. The outer diameter should be kept constant to prevent protrusions being formed on the shank of the post which interfere with atom probe data collection. Sample drift can also be a problem if this outer diameter is too small and can also cause these protrusions. Fig. 3 is an example of annular milling applied to an alloy, prepared using the micropost liftout technique (described in section 4.4.1 of this paper) where a Pt capping layer has been deposited at the tip.

For each mill, a schematic (not to scale) of the annular pattern, along with the ion current and inner radius of the mill are given. The un-milled post is shown in Fig. 3(a). This was subject to a 3 nA mill with an inner radius of 3 μm , as shown in the corresponding schematic. Upon polishing the composition of the post is revealed, in this case to show the alloy and Pt cap which has been applied during the post preparation. Progressively lower ion currents and inner radii are applied, some of which are shown in (b) and (c). The complete series of annular mills to produce this post and their respective ion currents and inner radii were: 3 nA and 3 μm , 1 nA and 1 μm , 0.5 nA and 0.5 μm , 0.1 nA and 0.3 μm , 0.1 nA and 0.2 μm .

Annular milling is known to change the structure and composition of the sample. For example a 30 kV annular mill has been observed to create an amorphous layer from a single crystal magnesium alloy sample 30 nm in from the sidewall of a (magnesium alloy) post [24] and implant significant amounts of Ga up to 50 nm into the surface [25]. A final stage of preparation of a micro-tip is low energy "clean up" milling following sharpening of the tip, usually at 5 kV or less, to remove this damaged layer [19, 25]. A 5 kV mill can reduce such an amorphous layer to < 5 nm and the maximum Ga-implantation depth to < 10 nm. This mill is normally performed as a solid (not annular) mill of the tip while being simultaneously monitored using the SEM of a dual beam FIB.

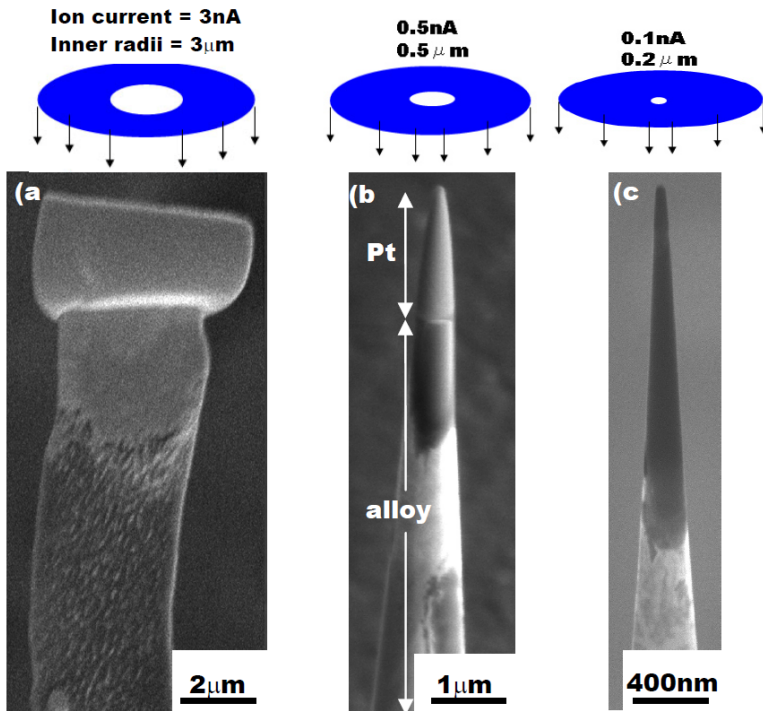


Fig. 3: The tip of the post during different stages of annular milling using a solid annulus pattern. The schematic (not to scale) indicates the typical inner radii dimension and ion current appropriate to mill the post beneath.

4. Micropost fabrication techniques

4.1 Moat method

The “moat method” initially places a platinum cap around the area of interest to protect it from stray ion damage, and then uses a large ion current beam (typically several nA) annular mill to create a deep trench (or “moat”) around the Pt cap leaving a needle of the appropriate dimensions [6, 23]. Edges of the moat must be wide and deep enough to allow the local electrode of the atom probe to distinguish the tip and to prevent field effects from the sidewalls interfering with the AP signal, typically 50-100 μm. An SEM image of a moat created using large ion current mills is seen in Fig. 4(a). Fig. 4(b) shows the tip of the post following annular milling ready for field ion evaporation in the atom probe. The major problem with this method is the time taken for the large initial mill and is therefore only suitable for conductive materials that mill easily, and where FIB beam time is sufficiently available (~1 day/sample).

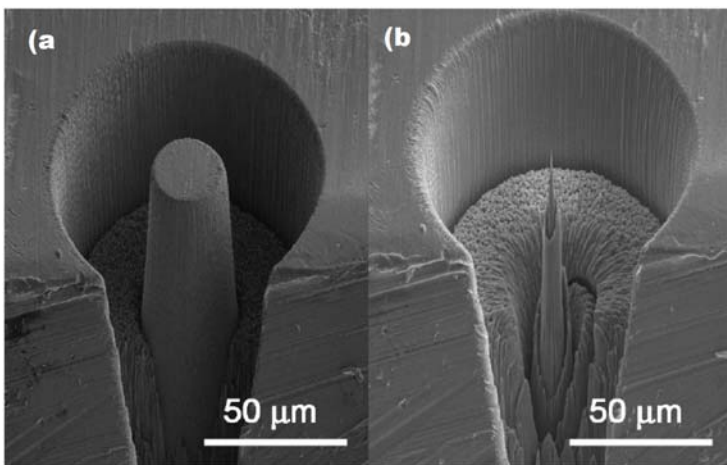


Fig. 4: The Moat method. SEM images showing the required steps to produce atom probe posts from a bulk specimen [6]. (a) Specimen following large ion current “moat” mill. (b) specimen following fine annular milling ready for atom probe analysis.

4.2 Wedge Method

The Wedge method, also known as the “cut out” method was one of the earlier FIB-based techniques to produce atom probe samples [26-27]. It addressed the major problem of milling large volumes of material, as is the case with the “Moat” method, and represented a technique with (a limited) degree of site selectivity making it a popular method to analyse the composition of grain boundaries (GB) in metals [26]. It was also the first technique developed which, in principle, allows a preliminary TEM examination of the region of interest.

The procedure involves mechanical polishing the sample to a thickness of around 10 μm using a tripod polisher to produce a wedge, such as that shown in Fig. 5(a). An area of interest (e.g. grain boundary) along the tip of the wedge is located and then marked by line cuts (in the positions of the dashed line in Fig. 5(a)). Pt is deposited over the area of interest before high beam current mill at the position of these line cuts remove the two triangular segments leaving a post. This post is then sharpened via annular milling ready for analysis as shown in Fig. 5(b).

This technique has the advantage of not requiring a pre-prepared post or a micro-manipulator, and allows for a prior TEM analysis. It is limited to conductive samples which are easily polished and, as a site-specific technique, to locations that can only (accurately) be chosen from the area within the polished wedge, that is the exterior of the specimen.

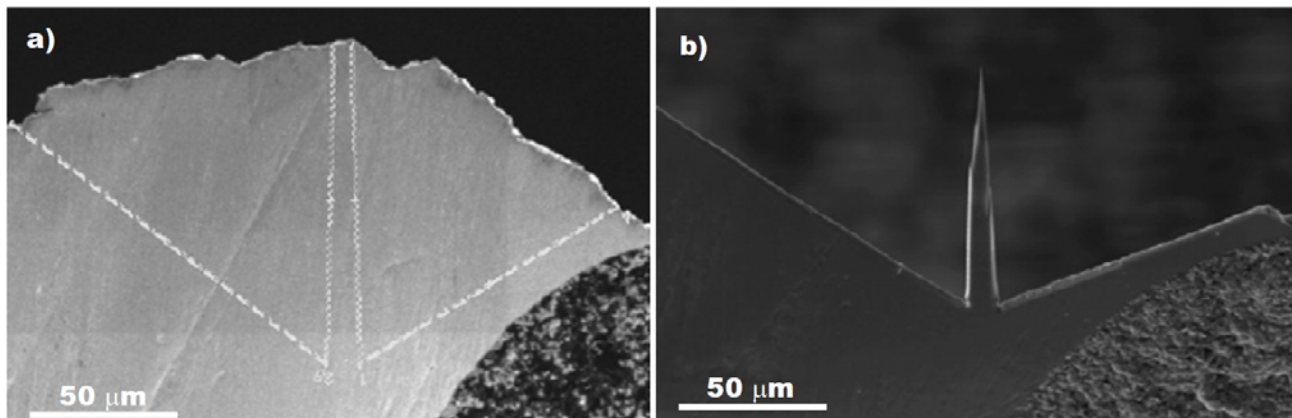


Fig. 5: The wedge method [27]. A conductive sample is mechanically polished to a thin wedge, then mounted in a FIB ready for line cuts in the positions indicated by the white lines in the SEM image (a). Following these mills the triangular sections are detached and the remaining post annular milled to a sharp tip ready for AP analysis, as shown in the SEM image (b).

4.3 Lift-out Method

The lift-out (or “coupon”) method has proven successful for the preparation of AP specimens, as it has been adopted by many authors since Dual Beam FIB systems became available with *in-situ* micromanipulators [6, 23, 25, 27-30].

The first step of the process involves a number of mills very similar to those used for the well established “lift-out” technique for TEM cross-section specimen preparation [31]. Trenches are dug via FIB milling leaving a ROI as a slice 3-5 μm in thickness, as shown in Fig. 6(a). The sample is tilted to perform mills that undercut the slice leaving it only attached at one edge. An “in-situ” micro-manipulator is inserted and maneuvered close ($< 0.5 \mu\text{m}$) to the sample. Gas chemistries (incorporated with many commercially available FIB systems) are used to perform a deposition (commonly Pt, W or a-C) attaching the needle to the ROI, as shown in Fig. 6 (b). The sample is then lifted out and maneuvered to a pre-prepared conductive post or (commercially available) micropost array using the micro-manipulator. The final step involves another deposition to attach the ROI to the post, and a mill to detach the ROI from the micromanipulator needle, as shown in Fig. 6(c). Variations include mounting on W tips [32] etched Si arrays of posts [25, 33] or optical mounting [34]. Finally, the sample is subject to annular milling to sharpen the tip.

A number of variations of the liftout technique have been published, such as the “backside” technique for a near surface ROI [14, 35], a protected liftout and mounting technique for nanowires [13, 36]. All use the same principle of FIB milling to detach the region of interest (ROI) from the bulk, lift-out using an in-situ micromanipulator, attachment to a pre-prepared post using FIB gas chemistries and finally sharpening by annular milling. This method is applicable to metallic and semiconductor systems, as illustrated in this article, and also to oxides and soft materials [37].

This is regarded as a most efficient FIB-based method of producing atom probe samples however it does have some limitations. The first is the requirement of an *in-situ* micromanipulator, which may not be readily available in many FIB laboratories. The second is the difficulty in preparing or obtaining suitably sharp conductive needles to mount the specimen on.

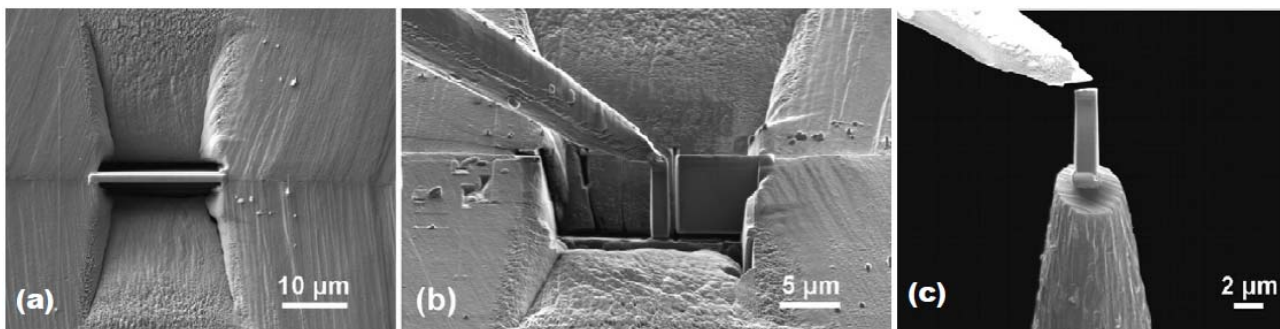


Fig. 6: The Lift-out technique [28]. (a) FIB milled trenches to expose the ROI. (b) The ROI is attached to a micromanipulator using a FIB deposition, and detached from the bulk using a series of FIB mills. (c) The ROI is moved from its cut-out location and to a pre-prepared tip, where it is welded using another FIB deposition.

4.4 Micropost Release Technique

The micropost release technique was developed initially as a means to produce site specific atom probe samples that did not require the use of an in-situ micromanipulator and allowed for a preliminary TEM analysis of the sharpened tip [38]. Since its development a number of variations have been published to suit specific applications, some of which are detailed later in this paper [24, 30].

The micropost release technique itself is outlined in Fig. 7. The initial step in the formation of a micro-post is a series of mills to produce the structure shown in Fig. 7(a). As an initial step a deposition (e.g. Pt, a-C or W) along the length of the post can be used to increase the bulk conductivity of the post and protect the sample from overspray of the ion beam. The first mills are “angled undercuts”, shown in Fig. 7(b), using line (or high aspect ratio rectangular) mills with the sample tilted $+45^\circ$ relative to the incident ion beam for the first, and then rotating it through 180° (which yields an equivalent orientation of -45° relative to the ion beam) to perform the second. The spacing and depth must be carefully chosen so that they intersect and the underside of the post is detached from the bulk (often an additional mill at is required in the position of the first angled under cut to release the post from re-deposited material which can re-weld the post to the base). A FIB cross-section in Fig. 7(b) shows the results of these angled undercuts. In order to release the ends of the micro-post, a regular cross-sectional mill, which produces “stair-case” type cuts was made with the ion beam incident normal to the material surface as indicated in Fig. 7(a).

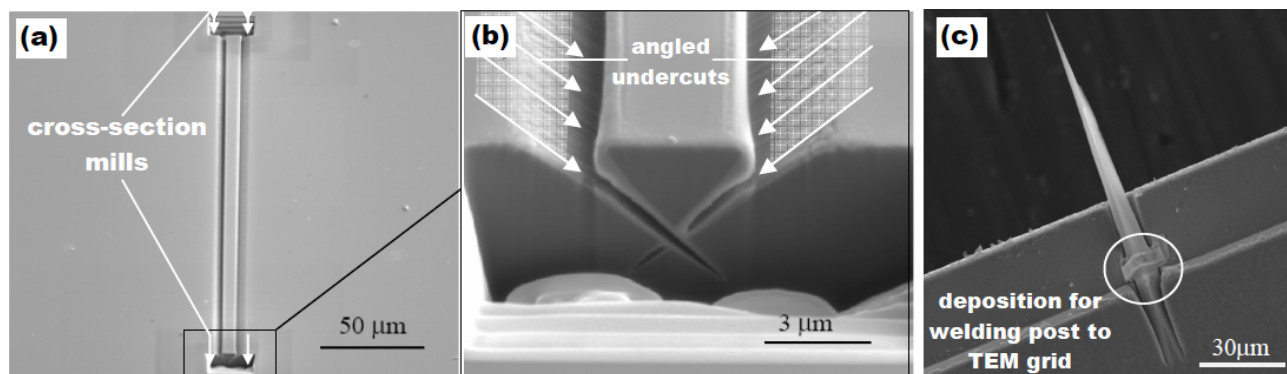


Fig. 7: Secondary electron images of the post ready to be lifted out [24]. (a) Low magnification SEM image showing the entire post and (b) close up of the cross section made to release the post. (c) the post after lift-out and welding onto a TEM grid, and annular milling, ready for TEM and atom probe analysis.

Dislodgment, and subsequent extraction, of the micro-post from the trench can be performed using either an ex-situ or in-situ micro-manipulator to maneuver the post to the edge of a TEM slot grid such as that shown in Fig. 7(c). For an in-situ micromanipulator this procedure is similar to that described for the “lift-out” method. For an *in-situ* micromanipulator, this extraction is very similar to the established technique for lifting out TEM specimen which attaches the post to a glass micromanipulator needle using electrostatic force [31]. The post/TEM slot is then placed back into the FIB where its base can be welded in place using a deposition, to produce a structure such as that shown in Fig. 7 (c). The post is then ready for annular milling to sharpen the tip for TEM analysis. After TEM analysis the Cu slot holding the specimen can be simply transferred to a Cu LEAP mount, for atom probe analysis.

Three examples of adaptations of the micropost release technique are described in the following sections. These examples demonstrate the use of traditional FIB techniques to obtain a select ROI at the tip of a micropost for APT analysis.

4.4.1 Cross section – sub-surface precipitate example

A basic function of a FIB and the fundamental concept behind the design of a dual beam FIB is its ability to perform mills into a sample's surface while sub-surface features can be imaged in real time. The Micro-post release technique allows FIB cross-sectioning to be combined with atom probe post fabrication, such that sub-surface features can be identified and preserved in an atom probe micro-post. A description of this technique is given in the following example.

We fabricated an atom probe tip at the interface between a crystalline precipitate in a bulk metallic glass (BMG) alloy ($\text{Mg}_{65}\text{Cu}_{25}\text{Y}_{10}$), which has provided valuable insight about the crystallisation behaviour of this system [24].

A crystallite was identified using a dual beam FIB cross section of an area under an irregularity in an otherwise smooth fracture surface of the BMG. Milling this cross-section included performing a higher current (e.g. 1 nA) “stair-case” like cut to mill to the appropriate depth, followed by lower current (e.g. 100 pA) “clean up” mills to smooth the section removing topographic artifacts, which would affect the clarity of the cross-sectional image. An SEM image of this cross section, as well as a higher magnification image of the crystallite in the amorphous bulk, can be seen in Fig. 8(a) and at a higher magnification in (b). These images reveal a crystallite several microns in size which appears darker than the surrounding amorphous BMG material.

In order to fabricate the atom probe post to contain such crystallites at the tip, the location of this larger crystallite was recorded. Fig. 8(a) shows the depth of the larger crystal from the surface ($2.7\text{ }\mu\text{m}$) and distance from the left side of the trench ($4.81\text{ }\mu\text{m}$). Once located, line mills were performed to mark the position of the crystal relative to the outer surface, as shown by the arrows in Fig. 8(c). The trench was then filled with Pt, and milled to a post according to ‘micropost liftout’ technique. Following the “angled undercut” mills the resulting post is shown in Fig. 8(d) with the tip positioned at the Pt deposition. Note that the mills were positioned to create a tapered post. In this instance, BMG samples are brittle and prone to mechanical failure in the high field environment of AP data collection [24]. This taper adds mechanical integrity to the post to reduce the chance of such failure. This sample was lifted out according to the micropost lift-out technique. Images of the various stages of annular milling for this sample are presented in Fig. 3, and a corresponding AP results shown in Fig. 1(b).

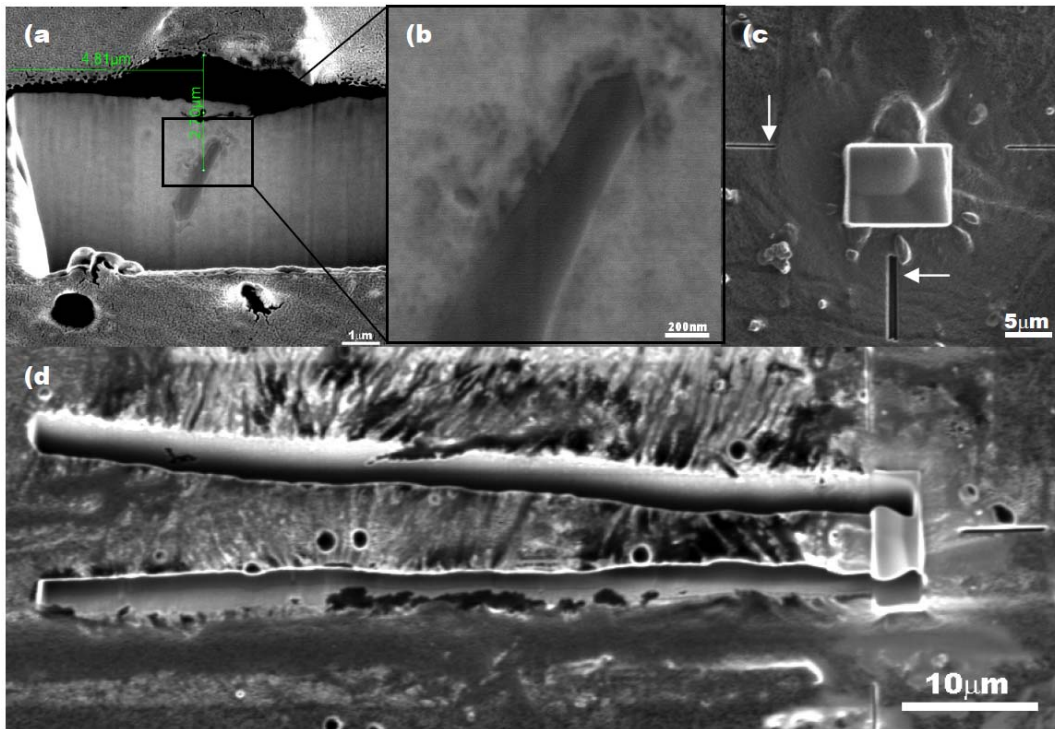


Fig. 8: The first stages of the production of the atom probe post from a crystallite contained within a glass phase magnesium bulk. (a) shows a secondary electron SEM image of a cross-section milled to reveal a sub-surface crystallite. This crystallite exhibits darker contrast and has its position identified by line measurements. (b) shows a higher magnification image of the crystallite in this cross-section. (c) shows alignment marks (white arrows) patterned to indicate the position of the sub-surface crystallite relative to the surface. (d) shows the post after mills ‘A’ and ‘B’ to produce the post with a tapered shank.

4.4.2 Ion channeling contrast - Cu-Bi alloy example

Ion channeling can be used as a contrast mechanism which discriminates between crystallographic orientations and, thus, can produce images of grain structure. In many materials ion channeling contrast can be seen directly by imaging a polished surface to reveal grain structure, or to identify a grain boundary (or other crystallographic features) as a location to fabricate an atom probe tip using the micro-post release technique. The exploitation of ion channeling contrast for a combined AP/TEM analysis is demonstrated by the example below analysing a planar defect in a Cu-Bi alloy.

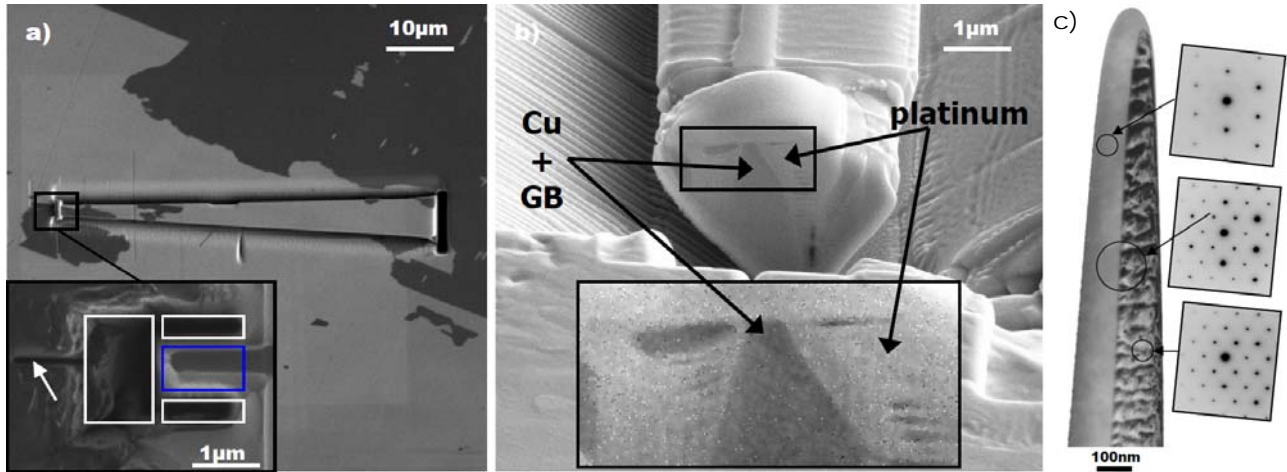


Fig. 9: (a) FIB image from a secondary electron signal showing ion channelling contrast taken from a Cu-Bi surface following “micropost release” cuts to produce the post. The inset shows milling of the tip used to isolate the ROI (b) SEM image of the end of the post containing the area of interest after it has been cut free from the bulk using regular ‘cross section mills’, and polished using ‘cleaning cross section’ mills. The areas of interest containing the grain boundary (“Cu + GB”), as well as surrounding deposited Pt exposed by these mills, are labelled. (c) TEM image and selected area electron diffraction patterns of a boundary and the material either side used to characterise the interface.

Fig. 9 (a) shows an ion beam induced secondary electron image of a polished surface from a Cu-Bi alloy where two different grains exhibit strong ion channeling contrast as identified by light and dark regions. The inset in (a) shows a higher resolution image of the area selected to produce the tip as it contained a grain boundary. An alignment marker, indicated by a white arrow, was patterned using the FIB to mark the position of a grain boundary identified from the ion image. Mills were then performed such that the selected grain boundary was contained in the area marked by the blue rectangle with its orientation parallel to the axis of the post. Three ion mills, shown by white rectangles in the inset in Fig. 9(a), removed material from the area immediately surrounding the grain boundary. The purpose of these mills was to reduce the cross-sectional area known to contain the grain boundary and to aid in the exact positioning of the annular milling such that the ROI could be contained in the final microtip. These trenches were later filled with platinum, in situ in the FIB, to protect the area of interest from damage during high ion current milling per the micro-post release technique. The resulting post prior to lift-out can be seen in Fig. 9(a).

A FIB polished cross-section of the ROI end of the post is shown in Fig. 9(b). The area of interest containing the grain boundary, as well as surrounding Pt, are indicated and can easily be distinguished. This provides a useful guide for positioning of annular milling to retain the grain boundary in the tip. Following the lift-out and annular milling procedures, the result, showing the grain boundary, can be seen by the bright field TEM image and corresponding selected area electron diffraction pattern shown in Fig. 9(c).

The grain boundary, as imaged in Fig. 9(c), appears to lie vertical relative to the axis of the post and parallel to the direction of the electron beam. The diffraction pattern to left of the boundary (upper diffraction pattern) is identified to be centered on the $\langle 114 \rangle$ zone axis of Cu. The lower diffraction pattern from the grain to the right side of the post indicating that the $\langle 110 \rangle$ zone axis. The middle diffraction pattern shows the SAED pattern over both grains which appear as a super position of the upper and lower diffraction patterns. These results suggest that the grains have a strong orientation relationship, a critical result in the study of this system.

4.4.3 Encapsulation method – semiconductor device example

The “Micropost release” technique has been adapted specifically for samples with insulating components or surroundings, or semiconductor devices which cannot easily be prepared by other means. This method, while adding an element of complexity relative to other techniques, is suited to the widest variety of samples as it isolates the ROI from its surrounding material. This method is called the encapsulation method and is explained via demonstration using a semiconductor (SC) device. A number of demonstrations of the capabilities of atom probe for semiconductor devices are given in literature [39-41].

The first step of this technique is similar to the well established method of milling TEM sections for ex-situ liftout [31] with the principal difference being that the foil is $< 1\ \mu\text{m}$ in thickness. Fig. 10(a) shows such a cross-section containing a semiconductor device which has been prepared using proprietary TEM scripts. Once detached from the bulk the foil is transferred via micromanipulation, and laid flat onto a conducting substrate which has sufficient strength and conductivity to act as a micro-post, a flat Cu-based alloy surface in this case.

This device was made from a silicon film on a substrate of sapphire. In order for a successful AP analysis this insulating sapphire had to be removed, and the device isolated such that annular milling could be centered on the ROI. As shown in Fig. 10(b) the device was isolated using a series of mills around the ROI, identified by the white box. This structure was then covered in platinum, as shown in Fig. 10(c) to protect the device from the high current mills to create the post according to the micropost release technique in the next step. These mills will be located in the position identified by the white lines and arrows. The “micro-post release” technique is then employed to produce a post comprising of the high conductivity copper surface with the area of interest encapsulated with platinum at the tip.

Following the “stair case” cuts to free the ends of the micropost (as per the micropost release technique), a cleaning cross-section was used to slowly polish the end of the post until contrast representing the edge of the ROI could be identified. In this example, the contrast became apparent when the surface produced by the cleaning cross section revealed silicon (as identified by energy dispersive X-ray analysis), indicating that the insulating sapphire layer was completely removed. This cross-section is shown in Fig. 10(d) with the device ROI circled. This surface could then be used as a guide to precisely position annular milling over the ROI to finish the micropost ready for TEM and AP analysis.

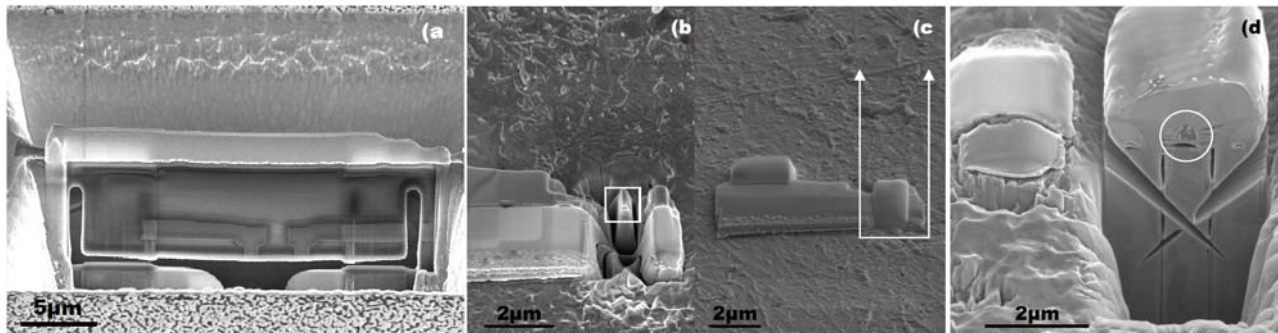


Fig. 10: Secondary electron images taken at different stages during the fabrication of an atom probe post of a semiconductor device on an insulating substrate. (a) FIB milled foil containing a semiconductor device (similar to a TEM cross section). (b) after the sample is lifted out (via micromanipulation) onto a conducting surface the area immediately surrounding the ROI (or device in this case, indicated by the white box) is milled away to remove any surrounding insulating material and isolate a small area containing the device. (c) shows this area after it was encapsulated with Pt. White lines indicate the approximate position of where the patterning will produce the end of the AP post. (d) a polished cross section of the end of the post after all mills are completed. This cross section intersects substrate very close to the device silicon. Compositional contrast in this image distinguishes the silicon in the ROI from the deposited Pt surrounding it, located within the white circle.

5. Summary

The focused ion beam has provided a means of sample preparation for most applications of atom probe tomography. Some of the first, the Moat, Wedge and Coupon techniques, evolved out of need to solve specific atom probe-based scientific problems at hand. This paper also presents a body of work surrounding the micropost liftout technique, a versatile method shown to produce atom probe posts [5], which can exploit a number of unique FIB capabilities to help identify and fabricate an ROI into an AP post.

This chapter gives an overview of the main techniques and where they can be applied. The descriptions are not exhaustive and are intended to be a starting point for anyone about to embark on an atom probe project. Table 1 provides a summary of these techniques, their application base, and a number of references for each.

Table 1: Summary of sample preparation techniques for Atom Probe Tomography

application	non-FIB	FIB based				FIB based - Micropost liftout		
	Electro-polishing	Annular milling	Moat	Wedge	Coupon	Ion Channeling	Cross section	Encapsulation
conductors	✓		✓	✓	✓	✓	✓	✓
insulators					✓	✓		✓
GB's			✓	✓	✓	✓	✓	✓
thin films					✓			✓
SC devices					✓			✓
sub surface				✓	✓		✓	✓
powders/particles					✓			✓
TEM analysis	✓			✓	✓	✓	✓	✓
References	8, 16	19-23, 25, 29	6, 23	27	13-14, 23, 25, 28-29, 32-37, 42	24	5, 38	24

References

- [1] Miller, M.K. and R.G. Forbes, *Atom probe tomography*. Materials Characterization, 2009. **60**(6): p. 461-469.
- [2] Miller, M.K., *Atom probe tomography : analysis at the atomic level*. 2000, London: Kluwer Academic/Plenum.
- [3] Tsong, T.T., *QUANTITATIVE SURFACE-ANALYSIS AT ATOMIC RESOLUTION, ATOM-PROBE FIELD-ION MICROSCOPY*. Journal of Vacuum Science & Technology a-Vacuum Surfaces and Films, 1990. **8**(4): p. 3397-3404.
- [4] Kelly, T.F. and M.K. Miller, *Invited review article: Atom probe tomography*. Review of Scientific Instruments, 2007. **78**(3).
- [5] Cairney, J., et al., *Recent Advances in FIB-based Site-specific Atom Probe Specimen Preparation Techniques*. Microscopy and Microanalysis, 2007. **13**(SupplementS02): p. 1634-1635.
- [6] Miller, M.K., *Sculpting Needle-Shaped Atom Probe Specimens with a Dual Beam FIB*. Microscopy and Microanalysis, 2005. **11**(SupplementS02): p. 808-809.
- [7] Arslan, I., et al., *Towards better 3-D reconstructions by combining electron tomography and atom-probe tomography*. Ultramicroscopy, 2008. **108**(12): p. 1579-1585.
- [8] Melmed, A.J. and J.J. Carroll, *An approach to realism in field ion microscopy via zone electropolishing*. Journal of Vacuum Science & Technology A: Vacuum, Surfaces, and Films, 1984. **2**(3): p. 1388-1389.
- [9] Ohno, Y., T. Kuroda, and S. Nakamura, *Atom-probe field-ion microscopy of GaAs and GaP*. Surface Science, 1978. **75**(4): p. 689-702.
- [10] Cerezo, A., C.R.M. Grovenor, and G.D.W. Smith, *PULSED LASER ATOM PROBE ANALYSIS OF GAAS AND INAS*. Applied Physics Letters, 1985. **46**(6): p. 567-569.
- [11] Nakamura, S., et al., *ATOM-PROBE ANALYSIS OF SIC*. Surface Science, 1986. **172**(3): p. L551-L554.
- [12] Melmed, A.J. and J.J. Carroll, *Feasibility of ToF atom-probe analysis of silicon*. Surface Science, 1981. **103**(2-3): p. L139-L142.
- [13] Xu, T., et al., *Growth of Si nanowires on micropillars for the study of their dopant distribution by atom probe tomography*. Journal of Vacuum Science & Technology B, 2008. **26**(6): p. 1960-1963.
- [14] Prosa, T., et al., *Backside Lift-Out Specimen Preparation: Reversing the Analysis Direction in Atom Probe Tomography*. Microscopy and Microanalysis, 2009. **15**(SupplementS2): p. 298-299.
- [15] Krakauer, B.W., et al., *A SYSTEM FOR SYSTEMATICALLY PREPARING ATOM-PROBE FIELD-ION-MICROSCOPE SPECIMENS FOR THE STUDY OF INTERNAL INTERFACES*. Review of Scientific Instruments, 1990. **61**(11): p. 3390-3398.
- [16] Krakauer, B.W. and D.N. Seidman, *SYSTEMATIC PROCEDURES FOR ATOM-PROBE FIELD-ION MICROSCOPY STUDIES OF GRAIN-BOUNDARY SEGREGATION*. Review of Scientific Instruments, 1992. **63**(9): p. 4071-4079.
- [17] Walls, J.M., E. Braun, and H.N. Southworth, *FIELD-ION MICROSCOPE OBSERVATIONS OF SPUTTERED TUNGSTEN SURFACES*. Japanese Journal of Applied Physics, 1974: p. 355-358.
- [18] Larson, D.J., et al., *FABRICATION OF MICROTIPS ON PLANAR SPECIMENS*. Applied Surface Science, 1995. **87-8**(1-4): p. 446-452.
- [19] Larson, D.J., et al., *Field-ion specimen preparation using focused ion-beam milling*. Ultramicroscopy, 1999. **79**(1-4): p. 287-293.
- [20] Larson, D.J., et al., *Advances in Atom Probe Specimen Fabrication from Planar Multilayer Thin Film Structures*. Microscopy and Microanalysis, 2001. **7**(01): p. 24-31.
- [21] Larson, D.J., et al., *Focused ion-beam milling for field-ion specimen preparation:: preliminary investigations*. Ultramicroscopy, 1998. **75**(3): p. 147-159.
- [22] Larson, D.J., et al., *Field ion specimen preparation from near-surface regions*. Ultramicroscopy, 1998. **73**(1-4): p. 273-278.
- [23] Miller, M.K., K.F. Russell, and G.B. Thompson, *Strategies for fabricating atom probe specimens with a dual beam FIB*. Ultramicroscopy, 2005. **102**(4): p. 287-298.
- [24] McKenzie, W.R., *PhD Thesis, School of Materials Science and Engineering*. 2007, University of New South Wales: Sydney.
- [25] Thompson, K., et al., *In situ site-specific specimen preparation for atom probe tomography*. Ultramicroscopy, 2007. **107**(2-3): p. 131-139.

- [26] Colijn, H.O., et al., *Site-Specific FIB Preparation of Atom Probe Samples*. Microscopy and Microanalysis, 2004. **10**(SupplementS02): p. 1150-1151.
- [27] Saxey, D.W., et al., *Atom probe specimen fabrication methods using a dual FIB/SEM*. Ultramicroscopy, 2007. **107**(9): p. 756-760.
- [28] Pérez-Willard, F., et al., *Focused ion beam preparation of atom probe specimens containing a single crystallographically well-defined grain boundary*. Micron, 2008. **39**(1): p. 45-52.
- [29] Miller, M.K. and K.F. Russell, *Atom probe specimen preparation with a dual beam SEM/FIB miller*. Ultramicroscopy, 2007. **107**(9): p. 761-766.
- [30] Cairney, J.M., et al., *Site-specific specimen preparation for atom probe tomography of grain boundaries*. Physica B: Condensed Matter, 2007. **394**(2): p. 267-269.
- [31] Giannuzzi, L.A. and F.A. Stevie, *A review of focused ion beam milling techniques for TEM specimen preparation*. Micron, 1999. **30**(3): p. 197-204.
- [32] Chen, Y.M., et al., *Laser-assisted atom probe analysis of zirconia/spinel nanocomposite ceramics*. Scripta Materialia, 2009. **61**(7): p. 693-696.
- [33] Morris, R.A., et al., *Fabrication of high-aspect ratio Si pillars for atom probe 'lift-out' and field ionization tips*. Ultramicroscopy, 2009. **109**(5): p. 492-496.
- [34] Thompson, G.B., M.K. Miller, and H.L. Fraser, *Some aspects of atom probe specimen preparation and analysis of thin film materials*. Ultramicroscopy, 2004. **100**(1-2): p. 25-34.
- [35] Gorman B. P., D.D., Salmon N., StachE., Amador G., Hartfield C. , *Hardware and Techniques for Cross-correlative TEM and Atom Probe Tomography*. Microscopy Today, 2008. **16**(4): p. 42.
- [36] Prosa, T., et al., *Analysis of Silicon Nanowires by Laser Atom Probe Tomography Prepared by a Protected Lift-Out Processing Technique*. Microscopy and Microanalysis, 2008. **14**(SupplementS2): p. 456-457.
- [37] Evans, J., et al., *3-D Atom Probe Tomography of Resin Embedded Samples?* Microscopy and Microanalysis, 2009. **15**(SupplementS2): p. 274-275.
- [38] McGrouther, D., et al., *Preparation of Site Specific Atom Probe Tips using Focused Ion Beam Technology*. Microscopy and Microanalysis, 2006. **12**(SupplementS02): p. 1296-1297.
- [39] Inoue, K., et al., *Dopant distributions in n-MOSFET structure observed by atom probe tomography*. Ultramicroscopy, 2009. **109**(12): p. 1479-1484.
- [40] Kelly, T.F., et al., *Atom probe tomography of electronic materials*. Annual Review of Materials Research, 2007. **37**: p. 681-727.
- [41] Moore, J.S., et al., *3-D analysis of semiconductor dopant distributions in a patterned structure using LEAP*. Ultramicroscopy, 2008. **108**(6): p. 536-539.
- [42] Choi, P.P., et al., *Application of focused ion beam to atom probe tomography specimen preparation from mechanically alloyed powders*. Microscopy and Microanalysis, 2007. **13**(5): p. 347-353.